Carbohydrate Polymers 102 (2014) 438–444

Contents lists available at ScienceDirect

Carbohydrate Polymers

journal homepage: www.elsevier.com/locate/carbpol

Characterisation of cellulose films regenerated from acetone/water coagulants

Hongjuan Geng[a], Zaiwu Yuan[a,b,**], Qingrui Fan[a], Xiaonan Dai[a], Yue Zhao[a], Zhaojiang Wang[a], Menghua Qin[c,*]

[a] Key Laboratory of Fine Chemicals in Universities of Shandong, Qilu University of Technology, Jinan 250353, China
[b] Key Laboratory of Colloid and Interface Chemistry, Ministry of Education, Shandong University, Jinan 250100, China
[c] Laboratory of Organic Chemistry, Taishan University, Taian 271021, China

ARTICLE INFO

Article history:
Received 25 September 2013
Accepted 28 November 2013
Available online 6 December 2013

Keywords:
Cellulose aqueous solutions
Regenerated cellulose films
Coagulation
Acetone
Slow release

ABSTRACT

A precooled aqueous solution of 7 wt% NaOH/12 wt% urea was used to dissolve cellulose up to a concentration of 2 wt%, which was then coagulated in an acetone/water mixture to regenerate cellulose film. The volume ratio of acetone to water (φ) had a dominant influence on film dimensional stability, film-forming ability, micromorphology, and mechanical strength. The film regenerated at $\varphi = 2.0$ showed excellent performance in both dimensional stability and film-forming ability. Compared to that from pure acetone, the cellulose film from the acetone/water mixture with $\varphi = 2.0$ was more densely interwoven, since the cellulosic fibrils formed during regeneration had pores with smaller average diameter. The alkali capsulated in the film during film formation could be released at quite a slow rate into the surrounding aqueous solution. The regenerated cellulose film with adjustable structure and properties may have potential applications in drug release and ultra filtration.

1. Introduction

Cellulose is well known as one of the world's most abundant and renewable natural resources (Armaroli & Balzani, 2006; Kim, Yun, & Ounaies, 2006; Klemm, Heublein, Fink, & Bohn, 2005; Mohanty, Misra, & Drzal, 2002; Turner, Spear, Holbrey, Daly, & Rogers, 2005). Due to its fascinating structure and excellent properties, such as fast biodegradability, environmental friendliness and good thermal stability, cellulose is increasingly regarded as one of the most promising raw materials for solving various problems, especially the oil crisis and environmental pollution (Goh, Tan, Lee, & Bhatia, 2010; Saxena, Adhikari, & Goyal, 2009; Scott, 1999). Cellulose use can be roughly classified into three aspects: direct use, degradation into small molecules and chemical modification based on its superstructure. In the biofuel field, a very promising treatment is to achieve the direct conversion of cellulose into long-chain polyols that imitate the components of petroleum (Fukuoka & Dhepe, 2006; Huber, Iborra, & Corma, 2006; Yan et al., 2006). A so-called 'green' chemical method known as acid hydrolysis in near-critical water combined with hydrogenation under a catalyst is attracting significant attention (Deng, Tan, Fang, Zhang, & Wang, 2009; Ji et al., 2008; Luo, Wang, & Liu, 2007; Zheng et al., 2009). Chemical modification, which provides a means of tuning the physical and chemical properties of cellulose to increase its functionality and broaden its application scope, plays a central role in cellulose application (John & Anandjiwala, 2007).

Direct use without any chemical derivation has also received considerable attention recently. The key challenge here is to disrupt the numerous inter- and intra-molecular H-bond networks among the chains of cellulose to make it soluble in desired solvents. Thus far, a few solvent systems for cellulose dissolution have been developed, including *N*,*N*-dimethylacetamide (DMAc)/LiCl, *N*-methylmorpholine *N*-oxide (NMMO) and some ionic liquids (Kulpinski, 2005; Liebert, Heinze, & Edgar, 2010; McCormick, Callais, & Hutchinson, 1985; Nishio & Manley, 1988; Rosenau et al., 2002). The textile fibres prepared from NMMO are called lyocell and exhibit outstanding performance such as regular circular cross sections, high crystallinity and excellent mechanical strength (Fink, Weigel, Purz, & Ganster, 2001). However, NMMO is expensive, unstable and difficult to recover. Ionic liquid is another attractive medium due to its non-volatility and easy recovery (Remsing, Swatloski, Rogers, & Moyna, 2006; Wu, Wang, Wang, Bian, & Li,

* Corresponding author at: Laboratory of Organic Chemistry, Taishan University, Taian 271021, China. Tel.: +86 538 8711009; fax: +86 538 6715521.
** Corresponding author at: Key Laboratory of Fine Chemicals in Universities of Shandong, Qilu University of Technology, Jinan 250353, China. Tel.: +86 531 89631208; fax: +86 531 89631111.
E-mail addresses: zwyuan163@163.com (Z. Yuan), qmh@qlu.edu.cn (M. Qin).

0144-8617/$ – see front matter © 2013 Elsevier Ltd. All rights reserved.
http://dx.doi.org/10.1016/j.carbpol.2013.11.071

2009; Zhu et al., 2006), but research in this direction is still in its infancy with a long way to go before industrial applications can be developed.

A new cellulose solvent known as the NaOH/urea/H_2O system has attracted increasing interest (Cai & Zhang, 2005, 2006; Cai et al., 2007, 2008; Chen et al., 2007; Fukuzumi, Saito, Iwata, Kumamoto, & Isogai, 2008; Guo, Zhou, & Zhang, 2011; Qi, Cai, Zhang, & Kuga, 2009; Weng, Zhang, Ruan, Shi, & Xu, 2004). In this system, only very cheap chemicals, such as NaOH and urea are adopted. The NaOH, urea and H_2O system needs to be precooled below −10 °C. Most importantly, no toxic substances are used or produced throughout the dissolving process, so it is considered a truly 'green' cellulose-dissolving method.

Cellulosic materials, including films, fibres and aerogels, can be regenerated from the cellulose aqueous solution by a variety of coagulants. A few studies have investigated the effects of coagulating conditions on the properties of the regenerated cellulose (RC) materials. Specifically, 5 wt% H_2SO_4/5 wt% Na_2SO_4 aqueous solutions are reported to be a good coagulant to achieve excellent mechanical properties (Zhang, Mao, Zhou, & Cai, 2005). Briefly, the RC materials are formed in coagulants mainly through the processes of ionic diffusion, primary-particle generation, secondary-particle growth and particle amalgamation (Inamoto, Iwata, Matsui, & Okajima, 1999; Inamoto, Miyamoto, Hongo, Iwata, & Okajima, 1996; Manabe, Kamata, Iijima, & Kamide, 1987).

In this study, we used a NaOH/urea/H_2O system to dissolve cellulose and an acetone/water mixture was selected as the coagulant to obtain RC films. The migration of NaOH from the cellulose solutions to the coagulants was investigated, and the capsulation and releasing behaviour of NaOH from the RC films were examined. The dimensional stability, structures, morphology and mechanical strength of the RC films were also studied. Our results are expected to provide valuable information on fabricating cellulosic materials, further expanding cellulose applications.

2. Experimental

2.1. Materials

The cellulose (cotton linter pulp) was supplied by China Silver Hawk Chemical Fibre Co., Ltd. (Gaomi, China). The average degree of polymerisation (DP) is 525. NaOH, urea and acetone were purchased from Sinopharm Chemical Reagent Co., Ltd. (Shanghai, China) and used without further purification. Double distilled water was used throughout the experiment.

2.2. Film preparation

As reported elsewhere (Cai & Zhang, 2005, 2006; Cai et al., 2007), an aqueous solution of 7 wt% NaOH/12 wt% urea was precooled to −12 °C in a refrigerator for 20 min, to which a known weight of native cellulose (NC) was dispersed with vigorous agitation for 5 min. The transparent cellulose solution was centrifuged at 4000 rpm for 10 min to remove the insoluble residuals and air bubbles. RC film was then prepared using a template method. Briefly, a mould was made using a tape frame stuck to a sheet of glass plate. The cellulose solution was then cast in the mould and immediately dipped into the coagulant for 5 min to obtain wet RC films. The chemicals remaining in the film were removed by thorough rinsing with deionised water. Finally, the film was dried at a constant temperature (30 °C) and humidity (65%) for 24 h.

2.3. Instrumental analysis

2.3.1. Acid–base titration and conductivity measurement

The amount of NaOH that migrated into the coagulant or stayed in the film was determined by acid–base titration against 0.1257 mol L^{-1} HCl with phenolphthalein as an indicator. A PHS-3C exact digital pH meter was used. The weight of the cellulose solution (2 wt%) was fixed at 1 g and the total volume of the coagulant was 20 mL. Conductivity measurements were performed on a conductivity meter, DDSJ-308A (China). First, the conductivity (κ) of 120 mmol L^{-1} NaCl was measured. Then, the κ of the same NaCl solution was measured with a wet or wetted RC film placed between the two platinum electrodes to inspect the barrier effect of the films on small ions.

2.3.2. Fourier transformation infrared (FT-IR) and wide-angle X-ray diffraction (WAXD) measurements

The FT-IR spectra of the dried RC films (ground into powders) were recorded on a Nexus 670 infrared spectrometer (Thermo-nicolet Electron Corporation, USA) using the KBr-disc method. WAXD analysis on the RC films was carried out by a conventional reflection method using a Cu Kα target at 40 kV and 30 mA. X-ray diffraction patterns were recorded in a 2θ range of 5–40°. The degree of crystallinity (χ_c) was calculated according to the peak separation method from the peak areas of the $(1\,\bar{1}\,0)$, $(1\,1\,0)$ and $(2\,0\,0)$ planes. The apparent crystal size (ACS) was estimated using Scherrer's equation (1):

$$\mathrm{ACS} = \frac{0.9\lambda}{\beta(\cos\theta)}, \tag{1}$$

with $\beta = (B^2 - b^2)^{1/2}$, where λ is the wavelength of the incident X-rays (1.5406 Å); θ is the diffraction angle corresponding to the $(1\,\bar{1}\,0)$, $(1\,1\,0)$ and $(2\,0\,0)$ planes; b is the instrumental constant (0.1°); and B is the half width in radians of the diffraction angle of the $(1\,\bar{1}\,0)$, $(1\,1\,0)$ and $(2\,0\,0)$ planes.

2.3.3. Transmission electron microscopy (TEM) and scanning electric microscopy (SEM) observation

A drop of 2 wt% cellulose solution was placed on a TEM grid (carbon grid, 3.02 mm, 200 meshes) with most of the liquid removed quickly using a piece of blotting paper, leaving a very thin film stretched over the grid. Thus, an ultra-thin RC film was formed by dipping it into a coagulant. The grid was then soaked in plenty of deionised water to remove the residual NaOH and urea. After staining by a 2% uranyl acetate aqueous solution, the grid was dried in ambient air for 60 min, followed by observation on a JEOL 100cx II TEM (Japan) at an accelerating voltage of 100 kV. For SEM observations, the RC film was fractured in liquid nitrogen and the fractured surface was then sputtered with gold and checked using a JEOL JMS-6700 SEM (Japan).

2.3.4. Surface tension measurements

Surface tensions (γ) at different cellulose concentrations were determined on a Processor Tensiometer K12 (Swiss) using a traditional Wilhelmy method.

2.3.5. Mechanical strength tests

The mechanical strength of the RC films (dimensions 0.4 cm × 5 cm with a thickness of 38–40 μm) was measured using a universal testing machine (Tianchen Testing Machine Manufacturing Co., Ltd., China) at a crosshead speed of 1 mm min^{-1}. A gauge length of 2 cm was used. To ensure data accuracy and reproducibility, at least five specimens were measured for each type of film.

All of the experiments were carried out at 20.0 ± 0.5 °C, unless otherwise stated.

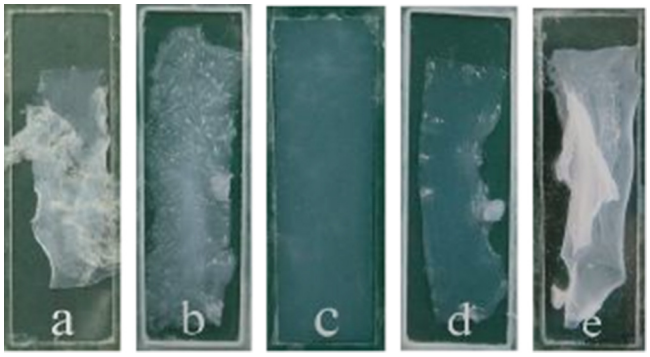

Fig. 1. Photographs of wet RC films regenerated from acetone/water mixtures with different φ: 0 (a), 0.5 (b), 2.0 (c), and ∞ (d), respectively. For comparison, a photograph of a wet RC film from 5 wt% H_2SO_4/Na_2SO_4 coagulant (e) is also shown.

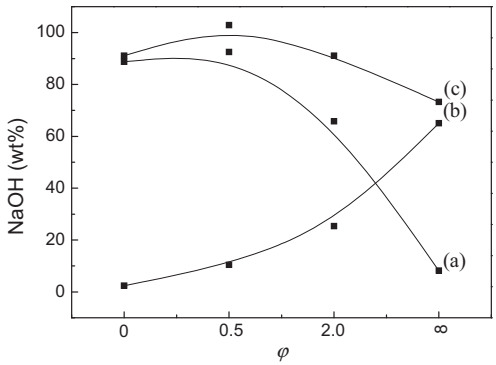

Fig. 2. Curves of NaOH percentage content: migrated into coagulants (a), kept in films (b), and the sum of the above two percentage contents (c) with increasing φ.

3. Results and discussion

3.1. Coagulating process and conditions

Based on the cellulose dissolution by the NaOH/urea/H_2O solvent, a few coagulant systems such as 5 wt % H_2SO_4/Na_2SO_4, Na_2SO_4, HOAc and $(NH_4)_2SO_4$ solutions have been investigated previously, among which 5 wt% H_2SO_4/Na_2SO_4 solution was evaluated as a good coagulant to prepare films with higher mechanical strength (Zhang et al., 2005). Using NaOH/urea/H_2O as the cellulose dissolving solvent, however, revealed that the acidic coagulant was not fully appreciated because both NaOH and H_2SO_4 were consumed due to the neutralisation reaction between them. Moreover, it is well known that NaOH readily absorbs CO_2 and produces $NaHCO_3$ or Na_2CO_3 when exposed to air, which will then react with H_2SO_4 during the coagulation procedure, leading to the formation and accumulation of CO_2 gas in RC films. This will inevitably influence the quality of the RC films. In addition, a relatively rapid reaction between OH^- and H^+ would lead to a very fast crystallisation of RC, which would lower the dimensional stability of the films.

To avoid the problems mentioned above, a non-reactive coagulant, *i.e.* acetone/water mixture, was chosen. Although a relatively low content of cellulose solution, *i.e.* 2 wt% more than a "concentrated" cellulose solution of up to 4 wt% (Zhang, Ruan, & Zhou, 2001), was selected, the dimensional stability of the RC film could still be achieved. The volume ratio of acetone to water (φ) was systematically changed and its influence on the dimensional stability of the RC film was checked. Fig. 1 summarises the appearance of six RC films prepared from different coagulants. When regenerated from pure water (*i.e.* $\varphi = 0$), the film has an irregular shape with a wrinkled and rough surface (Fig. 1a), indicating that in this condition, both the dimensional stability and film-forming ability are poor (normally, the smoothness of the surface of the film indicates the film-forming ability). When acetone was applied in the coagulant, the quality of the film improved, as seen in the film regenerated at $\varphi = 0.5$, although the film is still wrinkled (Fig. 1b). When φ was increased to 2.0, however, an RC film with a regular shape and smooth surface was obtained (Fig. 1c). A further increase of φ to ∞ (*i.e.* pure acetone) led to a decrease in the film quality (Fig. 1d). In a control experiment, RC film was also prepared using 5 wt% H_2SO_4/Na_2SO_4 as a coagulant. In this case, an RC film of low quality with a large number of entrapped CO_2 bubbles was obtained (Fig. 1e).

3.2. NaOH migration during coagulation

The investigation of NaOH migration is not only important for chemical recovery, but also crucial for the further elucidation of the coagulation mechanism. Driven by a high concentration gradient, NaOH will migrate from the cellulose solution to the coagulant, resulting in the formation of RC film. Finally, the migration rate of NaOH reaches equilibrium and the amount of NaOH in the film and in the coagulant no longer changes. Fig. 2 shows the weight percentage of migrated NaOH relative to its initial weight. Surprisingly, the extreme value does not appear at the side of pure water, but at $\varphi = 0.5$.

It could be deduced that the total amount of NaOH should be constant during the coagulation process because it was only a physical change. However, if the wet RC film were directly dried, *i.e.* without rinsing in deionised water, the calculated value of the total amount of NaOH was found to deviate from the theoretical amount. As shown in Fig. 2, the amount of NaOH migrating into the coagulant became smaller with increasing φ. This was probably due to the relatively low solubility of NaOH in acetone compared to water. In contrast, the NaOH that remained in the film increased gradually with φ. The sum of the above two at different φ is also shown in Fig. 2, from which one can see that the observed value of NaOH greatly deviated from the initial amount with increasing φ and goes so far as to decrease up to nearly 25 wt% at $\varphi = \infty$.

3.3. Slow-release effect of the RC films

In fact, the reduction in the total amount of NaOH should be attributed to the slow-release effect of hydroxyl ions, which induce the unreachable titration end-point in such a pH-indicator method. This assumption could be verified by a simple conductivity measurement. At $20.0 \pm 0.5\,^{\circ}C$, the conductivity (κ) of 120 mmol L^{-1} NaCl aqueous solution was measured to be 1.331 ms cm^{-1}. It would be slightly decreased to 1.316 ms cm^{-1} under the barrier of a 1 mm-thick wet RC film. This indicates that the wet RC film can hardly inhibit the mobility of small ions due to the existence of a large number of channels in the cellulose film. However, the RC film might be greatly compressed and the microstructure could become much denser after drying, resulting in a larger barrier effect on small ions in aqueous solution. Therefore, the corresponding κ continued to drop to 1.250 ms cm^{-1}. During acid–base titration, the mobility of small ions such as OH^- in the film was greatly suppressed, especially after drying, which accounted for the deviation of the total NaOH content mentioned above.

The slow release of small ions from the RC film could be further detected by a pH titration method, where the pH values were measured at regular time intervals during the acid-based titration. All of the pH titration curves at different φ reveal that at the beginning, the pH value dropped rapidly due to the quick acid–base neutralisation. With the further addition of HCl up to a pH range of 7–8, a platform appeared. This phenomenon differs greatly from that observed during a traditional acid–base titration in which the pH

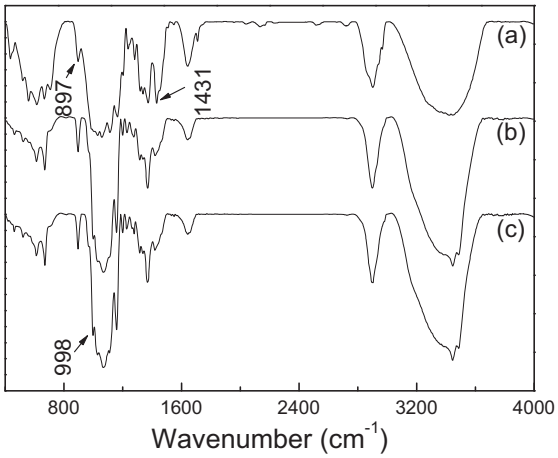

Fig. 3. FT-IR spectra of NC (a) and RC film without (b) and with (c) encapsulated NaOH.

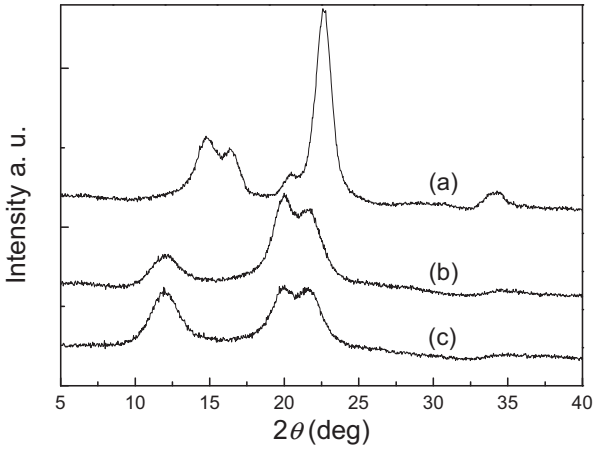

Fig. 4. XRD patterns for NC (a), RC film regenerated from a φ of 2.0 and via water-rinsing ((b) Film 3 in Table 1), and RC film from a φ of 2.0 without water-rinsing ((c) Film 3′ in Table 1).

value decreases quickly around pH = 7. This confirms the assumption that a part of NaOH does remain in the film, and is then released slowly into the surrounding medium. In addition, it is interesting that the slope of the titration curve at the initial stage became smaller and the platform was enlarged with increasing φ, indicating that the diffusion of ions was more hindered by the RC film at higher φ.

3.4. FT-IR and WAXD analysis

FT-IR was used to investigate the possible interaction between cellulose and NaOH. From Fig. 3, the FT-IR absorption band at 1431 cm^{-1} is assigned to CH_2 bending vibration, which is known as the "crystallinity band" in cellulose (Adsul, Soni, Bhargava, & Bansal, 2012). Compared to the NC, both of the RC films showed a significant reduction in the intensity of this band. While the absorption band at 897 cm^{-1} is assigned to the C—O—C stretching vibration at β-(1 → 4)-glycosidic linkages, which is considered an "amorphous band", the intensity of this band increased remarkably. Therefore, the intensity changes of FT-IR absorption in both crystalline and amorphous bands clearly suggests that the crystallinity was reduced after cellulose regeneration. However, the FT-IR spectra of the RC film with NaOH encapsulated were just the same as that without NaOH, except that the intensity of the C—O stretching vibration at 998 cm^{-1} was slightly higher. Thus, no chemical bonds between cellulose and NaOH were identified from FT-IR, indicating that NaOH was physically encapsulated in the cellulose films.

XRD measurement was performed to characterise the crystalline properties of the RC films. The X-ray diffraction pattern shown in Fig. 4 shows that the typical diffraction peaks of native cellulose (cellulose I) appeared at 22.6° (2 0 0), 16.4° (1 1 0) and 14.8° (1 $\bar{1}$ 0), respectively, which is consistent with the literature (Li et al., 2010; Zhang et al., 2001). For the RC film at φ = 2.0, however, the diffraction peaks appeared at 21.6° (2 0 0), 19.9° (1 1 0) and 12.0° (1 $\bar{1}$ 0), which indicates a crystal transition from cellulose I to cellulose II. Furthermore, the degree of crystallinity (X_c) of the dried RC film was greatly reduced compared to native cellulose. Table 1 gives the X_c and the apparent crystal size (ACS) at the different crystal planes of NC and four RC films, which were thoroughly rinsed with deionised water before drying. For comparison, the corresponding data on a film without water rinsing are also given. These data showed that the crystallinity of the cellulose is independent of the composition of the coagulant and the trapped NaOH. Therefore, the dimensional stability and film-forming ability is obviously independent of the crystal habit. However, the NaOH trapped in the film greatly altered the crystal size on different crystal planes. As shown in Table 1, the ACS on the (1 1 0) plane without water-rinsing increased, while the ACS on the (2 0 0) plane decreased compared to that with water-rinsing. It is possible that NaOH tends to physically adsorb on the (1 1 0) plane to selectively restrict the crystal growth.

3.5. Structural and morphological characterisations

It can be concluded from the above discussion that the slow release of NaOH from RC film is not a result of chemical adsorption, and thus it should be affected by the microstructure of the RC film. Therefore, it is interesting to study the microstructures of RC films at various φ through TEM and SEM observations. TEM images of the ultra-thin RC films coagulated at different φ (Fig. 5) reveal that the pore size distribution of each film varies obviously with φ. The film at φ = 2.0 had a much smaller averaged pore size than those of other films. It could be deduced that the cellulose molecules and their higher-order structures (*e.g.* microfibrils) were not liable to aggregate at φ = 2.0, which is further proven by the fact that the film prepared in this condition had the best quality among all of the films.

Surface tension is an important macroscopic property for both surfactant and polymer aqueous solutions, through which some microscopic information, such as molecular structure and aggregation behaviour can be obtained (Zhao & Zhu, 2003). It is believed that a stable inclusion complex consisting of NaOH, urea, water and cellulose is formed, leading to the dissolution of cellulose in the precooled NaOH/urea aqueous solution. In the theories of cellulose dissolution, urea is considered to function as a host, wrapping up the inclusion complex (Cai & Zhang, 2005; Mascal, Infantes, & Chisholm, 2005; Weng et al., 2004). Thus, it can be imagined that the

Table 1
Crystalline parameters of native cellulose and RC films. Films 1–4 represent the films prepared from φ of 0, 0.5, 2.0 and ∞, respectively. Film 3′ is the same as Film 3 but without water-rinsing.

Sample	Crystallinity (%)	ACS (Å)		
		1 $\bar{1}$ 0	1 1 0	2 0 0
Native cellulose	82	48	75	67
Film 1	64	35	47	55
Film 2	66	30	48	53
Film 3	67	33	40	54
Film 4	67	34	27	64
Film 3′	66	35	51	37

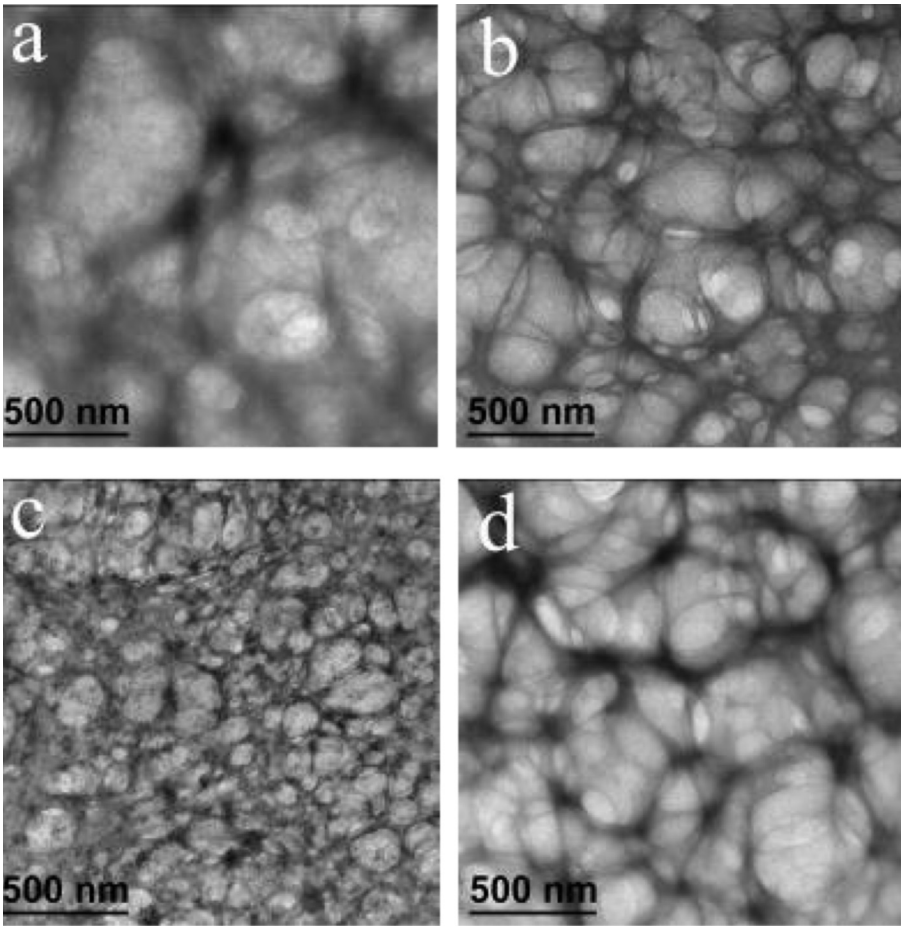

Fig. 5. TEM images of the ultra thin RC films coagulated at different φ: 0 (a), 0.5 (b), 2.0 (c), and ∞ (d), respectively.

existence of a cellulose complex would induce noticeable change in the surface properties of the aqueous solution. However, the surface tension (γ) of the NaOH/urea aqueous solution of cellulose has not been determined as far as we know. In this work, the surface tension was measured as a function of cellulose concentration (c_c). It is interesting that γ decreases continuously within the investigated c_c, indicating that the cellulose inclusion complex is surface active. Moreover, a turning point was noticed in the γ–c_c curve. In surfactant or amphiphilic polymer solutions (Zhao & Zhu, 2003), such a phenomenon is frequently seen and the turning point is thought to be the critical micelle/overlap concentration (*cmc* or c^*) of the soluble molecules, above which aggregates will form (Roy, Budtova, & Navard, 2003; Sovilj & Petrović, 2006; Tanaka, Meadows, Phillips, & Williams, 1990). We believe that the appearance of the turning point has a similar meaning, *i.e.* that cellulose molecular aggregates begin to form. As is known, the polarity of the coagulant becomes weaker with increasing φ. Considering the amphiphilicity of the cellulose complex, it could be deduced that the complex should be more compatible with the acetone/water mixture than pure water or acetone. At $\varphi = 2.0$, the polarity of the cellulose inclusion complex probably matches that of the coagulant. In that case, the cellulose higher-order structures (fibrils) could stretch to a larger extent when regenerated, resulting in a denser interwoven structure. In the condition in which φ deviates from 2.0, however, cellulose molecules tend to aggregate quickly, resulting in the formation of large clusters, as evidenced in Fig. 5a, b and d.

The structural and morphological characteristics of the RC films were further investigated by SEM. Consistent with the TEM results, SEM showed that the RC film at $\varphi = 2.0$ was more densely organised than others (Fig. 6). Further observations indicated that the granular clusters in RC film became smaller with the increase in φ. In particular, typical fibril-like ordered structures were observed at $\varphi = 2.0$, but they changed back to granular clusters when pure acetone was adopted as the coagulant. Evidently, it is easier for the cellulose molecules to aggregate in pure water than in the other three coagulants, leading to the serious film shrinkage responsible for poor film-forming ability. In the case of $\varphi = 2.0$, a transient compatibility between the amphiphilic cellulose inclusion complex and the coagulant formed before the film was regenerated allowed the cellulose chains to stretch to a larger extent.

3.6. Mechanical properties of RC films

Due to microstructural differences, the RC films showed different mechanical properties. Fig. 7 shows that both the tensile strength (σ) and the strain to failure (ε) were the lowest for the film at $\varphi = 0.5$, while the film at $\varphi = 2.0$ represented a greater ε and that at $\varphi = \infty$ had a larger σ. Because regular RC film could not be regenerated from pure water, the stress data for that circumstance is not shown here. It can be deduced that for the RC film at $\varphi = 2.0$, the larger ε probably originated from the more stretched structure of cellulose chains. However, the granular and homogeneous aggregate structure was favourable for the strength property of the film. For films at $\varphi = 0$ and 0.5, the aggregate was larger and polydisperse, which was believed to be the reason for a very low mechanical strength. However, for the film obtained from pure acetone, the greatest mechanical strength was achieved due to the formation of the moderate and homogeneous granular clusters.

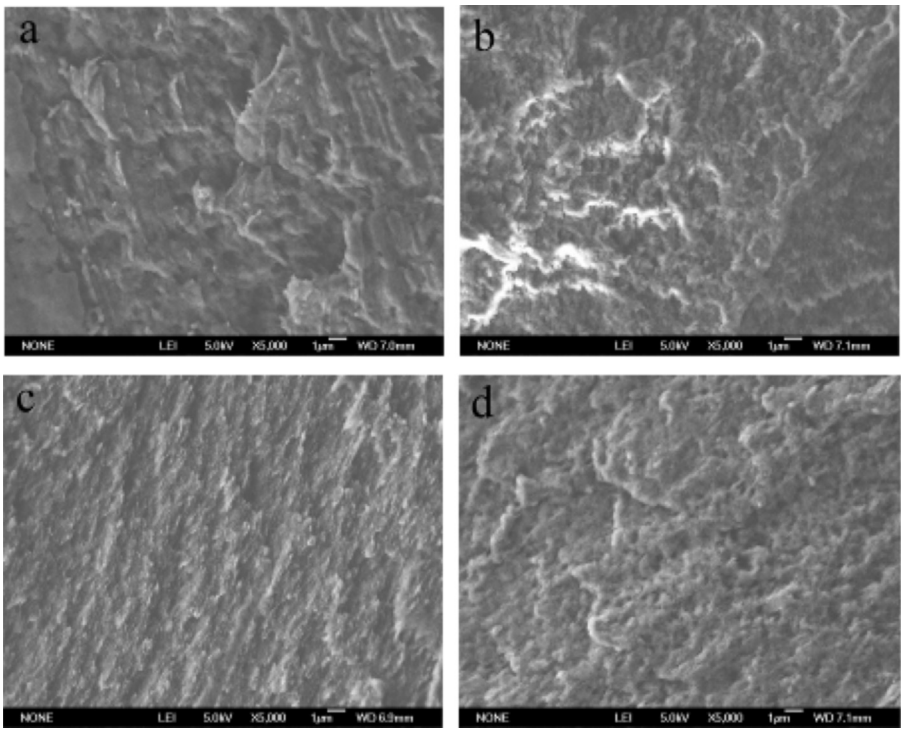

Fig. 6. SEM images of cross-sections of RC films coagulated from a variety of coagulants with φ of 0 (a), 0.5 (b), 2.0 (c) and ∞ (d), respectively.

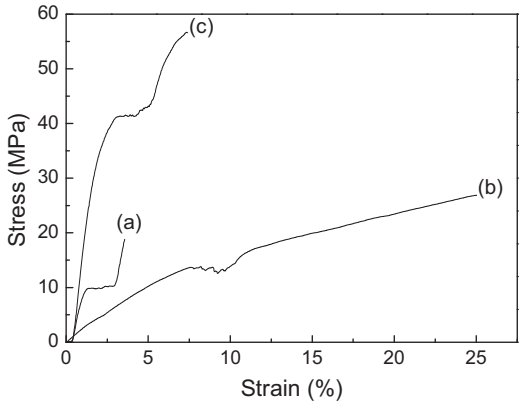

Fig. 7. The stress-strain curves of RC films regenerated from φ of 0.5 (a), 2.0 (b) and ∞ (c), respectively.

4. Conclusions

RC films were prepared using precooled 7 wt% NaOH/12 wt% urea as cellulose dissolving solvent and an acetone/water mixture with different volume ratios as coagulants. The dried RC films have a distinct slow-release effect on small ions, such as Na^+ and OH^-, in aqueous solution. This is attributed to the small pore size of the film, which induces a so-called capillary effect. The degree of crystallinity is similar for all RC films at different φ, but the apparent crystal size varies due to the selective adsorption of NaOH on specific crystal planes. The microstructure and mechanical properties of the RC films reveal an obvious dependence on φ. At $\varphi = 2.0$, a densely interwoven fibril-like structure is formed in the RC film, which is responsible for a higher strain to failure, whereas homogeneous granular morphology tends to be fabricated at higher φ, leading to a higher tensile strength. The results shown here are expected to provide a better understanding of both fundamental and practical applications of cellulose.

Acknowledgements

The authors would like to thank the China Postdoctoral Science Foundation (2012M511491) and Shandong Province Young and Middle-Aged Scientists Research Awards Fund (BS2012CL030), the National Natural Science Foundation of China (31370581) and the Program for the Scholar of Yellow River Mouth (DYRC20120105) for financial support.

Appendix A. Supplementary data

Supplementary data associated with this article can be found, in the online version, at http://dx.doi.org/10.1016/j.carbpol.2013.11.071.

References

Adsul, M., Soni, S. K., Bhargava, S. K., & Bansal, V. (2012). A facile approach for the dispersion of regenerated cellulose in aqueous system in the form of nanoparticles. *Biomacromolecules*, *13*, 2890–2895.

Armaroli, N., & Balzani, V. (2006). The future of energy supply: Challenges and opportunities. *Angewandte Chemie International Edition*, *46*, 52–66.

Cai, J., & Zhang, L. (2005). Rapid dissolution of cellulose in LiOH/urea and NaOH/urea aqueous solutions. *Macromolecular Bioscience*, *5*, 539–548.

Cai, J., & Zhang, L. (2006). Unique gelation behavior of cellulose in NaOH/urea aqueous solution. *Biomacromolecules*, *7*, 183–189.

Cai, J., Zhang, L., Chang, C., Cheng, G., Chen, X., & Chu, B. (2007). Hydrogen-bond-induced inclusion complex in aqueous cellulose/LiOH/urea solution at low temperature. *ChemPhysChem*, *8*, 1572–1579.

Cai, J., Zhang, L., Liu, S., Liu, Y., Xu, X., Chen, X., et al. (2008). Dynamic self-assembly induced rapid dissolution of cellulose at low temperatures. *Macromolecules*, *41*, 9345–9351.

Chen, X., Burger, C., Wan, F., Zhang, J., Rong, L., Hsiao, B. S., et al. (2007). Structure study of cellulose fibers wet-spun from environmentally friendly NaOH/urea aqueous solutions. *Biomacromolecules*, *8*, 1918–1926.

Deng, W., Tan, X., Fang, W., Zhang, Q., & Wang, Y. (2009). Conversion of cellulose into sorbitol over carbon nanotube-supported ruthenium catalyst. *Catalysis Letters*, *133*, 167–174.

Fink, H. P., Weigel, P., Purz, H., & Ganster, J. (2001). Structure formation of regenerated cellulose materials from NMMO-solutions. *Progress in Polymer Science*, *26*, 1473–1524.

Fukuoka, A., & Dhepe, P. L. (2006). Catalytic conversion of cellulose into sugar alcohols. *Angewandte Chemie International Edition*, *45*, 5161–5163.

Fukuzumi, H., Saito, T., Iwata, T., Kumamoto, Y., & Isogai, A. (2008). Transparent and high gas barrier films of cellulose nanofibers prepared by TEMPO-mediated oxidation. *Biomacromolecules*, *10*, 162–165.

Goh, C. S., Tan, K. T., Lee, K. T., & Bhatia, S. (2010). Bio-ethanol from lignocellulose: Status, perspectives and challenges in Malaysia. *Bioresource Technology*, *101*, 4834–4841.

Guo, Y., Zhou, J., & Zhang, L. (2011). Dynamic viscoelastic properties of cellulose carbamate dissolved in NaOH aqueous solution. *Biomacromolecules*, *12*, 1927–1934.

Huber, G. W., Iborra, S., & Corma, A. (2006). Synthesis of transportation fuels from biomass: Chemistry, catalysts, and engineering. *Chemical Reviews*, *106*, 4044–4098.

Inamoto, M., Iwata, M., Matsui, T., & Okajima, K. (1999). Morphological and structural formation of the regenerated cellulose membranes recovered from its cuprammonium solution using aqueous sulfuric acid. *Journal of Applied Polymer Science*, *72*, 1669–1678.

Inamoto, M., Miyamoto, I., Hongo, T., Iwata, M., & Okajima, K. (1996). Morphological formation of the regenerated cellulose membranes recovered from its cuprammonium solution using various coagulants. *Polymer Journal*, *28*, 507–512.

Ji, N., Zhang, T., Zheng, M., Wang, A., Wang, H., Wang, X., et al. (2008). Direct catalytic conversion of cellulose into ethylene glycol using nickel-promoted tungsten carbide catalysts. *Angewandte Chemie International Edition*, *120*, 8638–8641.

John, M. J., & Anandjiwala, R. D. (2007). Recent developments in chemical modification and characterization of natural fiber-reinforced composites. *Polymer Composites*, *29*, 187–207.

Kim, J., Yun, S., & Ounaies, Z. (2006). Discovery of cellulose as a smart material. *Macromolecules*, *39*, 4202–4206.

Klemm, D., Heublein, B., Fink, H. P., & Bohn, A. (2005). Cellulose: Fascinating biopolymer and sustainable raw material. *Angewandte Chemie International Edition*, *44*, 3358–3393.

Kulpinski, P. (2005). Cellulose nanofibers prepared by the N-methylmorpholine-N-oxide method. *Journal of Applied Polymer Science*, *98*, 1855–1859.

Li, R., Chang, C., Zhou, J., Zhang, L., Gu, W., Li, C., et al. (2010). Primarily industrialized trial of novel fibers spun from cellulose dope in NaOH/urea aqueous solution. *Industrial & Engineering Chemistry Research*, *49*, 11380–11384.

Liebert, T., Heinze, T., & Edgar, K. J. (2010). *Cellulose solvents: For analysis, shaping and chemical modification*. Washington, DC: American Chemical Society.

Luo, C., Wang, S., & Liu, H. (2007). Cellulose conversion into polyols catalyzed by reversibly formed acids and supported ruthenium clusters in hot water. *Angewandte Chemie International Edition*, *46*, 7636–7639.

Manabe, S. I., Kamata, Y., Iijima, H., & Kamide, K. (1987). Some morphological characteristics of porous polymeric membranes prepared by micro-phase separation method. *Polymer Journal*, *19*, 391–404.

Mascal, M., Infantes, L., & Chisholm, J. (2005). Water oligomers in crystal hydrates – What's news and what isn't? *Angewandte Chemie International Edition*, *45*, 32–36.

McCormick, C. L., Callais, P. A., & Hutchinson, B. H., Jr. (1985). Solution studies of cellulose in lithium chloride and *N*,*N*-dimethylacetamide. *Macromolecules*, *18*, 2394–2401.

Mohanty, A., Misra, M., & Drzal, L. (2002). Sustainable bio-composites from renewable resources: Opportunities and challenges in the green materials world. *Journal of Polymers and the Environment*, *10*, 19–26.

Nishio, Y., & Manley, R. S. J. (1988). Cellulose–poly(vinyl alcohol) blends prepared from solutions in *N*,*N*-dimethylacetamide-lithium chloride. *Macromolecules*, *21*, 1270–1277.

Qi, H., Cai, J., Zhang, L., & Kuga, S. (2009). Properties of films composed of cellulose nanowhiskers and a cellulose matrix regenerated from alkali/urea solution. *Biomacromolecules*, *10*, 1597–1602.

Remsing, R. C., Swatloski, R. P., Rogers, R. D., & Moyna, G. (2006). Mechanism of cellulose dissolution in the ionic liquid 1-*n*-butyl-3-methylimidazolium chloride: A ^{13}C and $^{35/37}Cl$ NMR relaxation study on model systems. *Chemical Communications*, *27*, 1271–1273.

Rosenau, T., Potthast, A., Adorjan, I., Hofinger, A., Sixta, H., Firgo, H., et al. (2002). Cellulose solutions in *N*-methylmorpholine-*N*-oxide (NMMO) – degradation processes and stabilizers. *Cellulose*, *9*, 283–291.

Roy, C., Budtova, T., & Navard, P. (2003). Rheological properties and gelation of aqueous cellulose-NaOH solutions. *Biomacromolecules*, *4*, 259–264.

Saxena, R., Adhikari, D., & Goyal, H. (2009). Biomass-based energy fuel through biochemical routes: A review. *Renewable and Sustainable Energy Reviews*, *13*, 167–178.

Scott, G. (1999). *Polymers and the environment*. London: Royal Society of Chemistry.

Sovilj, V. J., & Petrović, L. B. (2006). Influence of hydroxypropylmethyl cellulose–sodium dodecylsulfate interaction on the solution conductivity and viscosity and emulsion stability. *Carbohydrate Polymers*, *64*, 41–49.

Tanaka, R., Meadows, J., Phillips, G., & Williams, P. (1990). Viscometric and spectroscopic studies on the solution behaviour of hydrophobically modified cellulosic polymers. *Carbohydrate Polymers*, *12*, 443–459.

Turner, M. B., Spear, S. K., Holbrey, J. D., Daly, D. T., & Rogers, R. D. (2005). Ionic liquid-reconstituted cellulose composites as solid support matrices for biocatalyst immobilization. *Biomacromolecules*, *6*, 2497–2502.

Weng, L., Zhang, L., Ruan, D., Shi, L., & Xu, J. (2004). Thermal gelation of cellulose in a NaOH/thiourea aqueous solution. *Langmuir*, *20*, 2086–2093.

Wu, R. L., Wang, X. L., Wang, Y. Z., Bian, X. C., & Li, F. (2009). Cellulose/soy protein isolate blend films prepared via room-temperature ionic liquid. *Industrial & Engineering Chemistry Research*, *48*, 7132–7136.

Yan, N., Zhao, C., Luo, C., Dyson, P. J., Liu, H., & Kou, Y. (2006). One-step conversion of cellobiose to C_6-alcohols using a ruthenium nanocluster catalyst. *Journal of the American Chemical Society*, *128*, 8714–8715.

Zhang, L., Mao, Y., Zhou, J., & Cai, J. (2005). Effects of coagulation conditions on the properties of regenerated cellulose films prepared in NaOH/urea aqueous solution. *Industrial & Engineering Chemistry Research*, *44*, 522–529.

Zhang, L., Ruan, D., & Zhou, J. (2001). Structure and properties of regenerated cellulose films prepared from cotton linters in NaOH/urea aqueous solution. *Industrial & Engineering Chemistry Research*, *40*, 5923–5928.

Zhao, G. X., & Zhu, B. Y. (2003). *Principles of surfactant action*. Beijing: China Light Industry Press.

Zheng, M. Y., Wang, A. Q., Ji, N., Pang, J. F., Wang, X. D., & Zhang, T. (2009). Transition metal–tungsten bimetallic catalysts for the conversion of cellulose into ethylene glycol. *ChemSusChem*, *3*, 63–66.

Zhu, S., Wu, Y., Chen, Q., Yu, Z., Wang, C., Jin, S., et al. (2006). Dissolution of cellulose with ionic liquids and its application: A mini-review. *Green Chemistry*, *8*, 325–327.